Modeling of Surface Acoustic Wave Strain Sensors using Coupling-of-Modes Analysis

Brian Mc Cormack, *Graduate Student Member, IEEE,* Dermot Geraghty, and Margaret O'Mahony

***Abstract*—Surface Acoustic Wave (SAW) devices may be configured as strain sensors, providing passive, wireless strain measurement in demanding conditions. A key consideration is the modeling of the sensors, enabling different device designs to be considered. This paper presents a simulation scheme using Coupling-of-Modes (COM) analysis which allows both the frequency response of a SAW strain sensor and its bias sensitivity to be evaluated. Example applications are presented to demonstrate the use of the model.**

***Index Terms*—Coupled mode analysis, strain measurement, surface acoustic wave devices.**

I. Introduction

SURFACE Acoustic Wave (SAW) devices have been used for many years in RF communications as filters and delay lines. In recent times, their potential as wireless sensors has begun to be exploited [1]. Applications in torque measurement [2] and automotive monitoring [3], [4] (among other fields) have demonstrated their superiority over traditional sensor solutions. The passive, wireless nature of the devices is a key advantage not only in improving current measurement systems but also in enabling new applications which were previously impractical or impossible.

An important issue with SAW sensors is the modeling of the sensor response both to the interrogation signal and to applied biases (mechanical, electrical, magnetic etc.). As illustrated above, SAW devices are increasingly being used in wireless multi-sensor systems, where both the identity and measurand of each device must be uniquely determined. The simulation of such systems therefore requires both the detailed frequency response of a given sensor (for identification purposes) and its sensitivity to biases. Such modeling allows individual sensor designs to be evaluated at the design stage, and can also be used to estimate the behavior of the measurement system as a whole.

The accurate simulation of any SAW device is dependent upon knowledge of both the general wave behavior and the influence of the device's structures (IDTs, reflector gratings etc.) on these waves. Surface waves propagating in biased piezoelectric substrates may be considered as small fields superposed on biased electroelastic media [5]; this approach was first applied to surface waves subject to biasing stresses [6]. The effect of arbitrary (possibly inhomogeneous) small biases may be evaluated using a perturbation procedure [7]. This technique has been used to investigate a variety of biases on SAW device performance (e.g., [8], [9]), including a recent study on the pressure and temperature sensitivities of different piezoelectric substrates and cuts [10].

A wide variety of device models have been used to simulate the transduction and reflection of surface waves by SAW device structures [11], [12]. SAW sensors for strain or pressure measurement frequently use thin-film resonant designs with Rayleigh waves, and for these devices the Coupling-of-Modes (COM) formulation can provide excellent predictions of the unbiased device behavior [13]. COM modeling has recently been introduced for multi-layer liquid [14] and pressure sensors [15].

The integration of both of the general frequency response of a sensor and its bias sensitivity in a single model would be advantageous. For wireless SAW sensors, the measurand is inferred from the biased frequency response of the remote device. This response is determined by both the biased device design (which may be deformed from its original dimensions) and the biased surface wave; wireless interference effects may also be significant, but are not considered in this work. While evaluation of the wave behavior alone may be sufficient for some SAW sensors, particularly those with non-reflective structures, many designs also require that the biased device behavior be simulated. This is particularly important for sensor design, as devices optimized for resonant performance (e.g., in substrate type, SAW propagation direction etc.) may display suboptimal sensitivities as sensors: this will be discussed in Section III. Another benefit of integrated models is the ease with which they can be used as components within multi-sensor simulations. The effect of arbitrary biases (within the model's definition) may be easily applied within such simulations, allowing the evaluation of the sensor response(s) within the measurement system. For example, the achievable sensor resolution within a noisy RF channel could be evaluated. Conversely, the same integrated model could be used during the sensor design stage to optimize sensitivity to particular biases. This could be useful, for example, where the measurands are small or high selectivity is required.

This paper demonstrates how COM analysis can be used as an integrated modeling tool for SAW strain sensors [16]. The COM formulation is introduced in Section II, while the model parameters are discussed in Section III. An example application is given in Section IV to demonstrate the use of

Manuscript received February 27, 2008. This work was supported by the Higher Education Authority under the Programme for Research in Third-Level Institutions.

B. Mc Cormack and D. Geraghty are with the Department of Mechanical and Manufacturing Engineering, Trinity College, Dublin, Ireland e-mail: mccormb@tcd.ie.

M. O'Mahony is with the Department of Civil, Structural and Environmental Engineering, Trinity College, Dublin, Ireland.

the model, while conclusions are presented in Section V.

II. COM MODEL

COM analysis may be used to model wave propagation in many types of periodic media [17]. It describes the interaction between incident and reflected waves in a perturbed region: for SAW devices this coupling normally occurs in IDT and reflector grating structures. The formulation has several advantages over other techniques for sensor modeling:

- *Transparent, modular structure*: COM offers arguably the most natural approach to SAW sensor modeling, representing the device response in terms of wave coupling rather than discrete components, as is the case with equivalent circuits [18]. This is especially true for resonant devices, where the interactions between incident and reflected SAW are crucial to device operation. Its modular structure allows different device configurations to be easily tested.
- *Accurate simulation of narrowband devices*: many modern SAW sensors are implemented as narrowband Rayleigh wave devices with weak coupling, and the COM approach is very accurate for these components.
- *Small computational requirements*: in many cases analytical solutions can be obtained for device parameters, thus enabling the fast processing of simulations.

The primary disadvantage is one shared with other phenomenological models, namely that accurate independent parameters are required: these will be discussed in Section III. In a narrow frequency range around the nominal center frequency $f_0 = v/2p$ of a SAW structure, the wave fields at position x_1 along the propagation direction may be approximated by [13]:

$$\begin{aligned}\frac{\mathrm{d}R(x_1)}{\mathrm{d}x_1} &= -\mathrm{i}\delta R(x_1) + \mathrm{i}\kappa S(x_1) + \mathrm{i}\alpha V \\ \frac{\mathrm{d}S(x_1)}{\mathrm{d}x_1} &= -\mathrm{i}\kappa^* R(x_1) + \mathrm{i}\delta S(x_1) - \mathrm{i}\alpha^* V \\ \frac{\mathrm{d}I(x_1)}{\mathrm{d}x_1} &= -2\mathrm{i}\alpha^* R(x_1) - 2\mathrm{i}\alpha S(x_1) + \mathrm{i}\omega C V\end{aligned} \tag{1}$$

In the coupled equations above, $R(x_1)$ and $S(x_1)$ are the slowly-varying wave fields, $I(x_1)$ is the IDT current, $\delta = 2\pi(f - f_0)/v - \mathrm{i}\gamma$ is the detuning parameter, ω is the angular frequency and V is the applied voltage. The remaining variables represent the parameters which must be independently determined:

- The effective SAW velocity v
- The SAW attenuation γ
- The electrode reflectivity κ
- The transduction coefficient α
- The capacitance C

Asterisks in the above variables denote complex conjugation. Fig. 1 shows some of the above quantities, with $\psi_+(x_1) = R(x_1)\mathrm{e}^{-\mathrm{i}\pi x_1/p}$ and $\psi_-(x_1) = S(x_1)\mathrm{e}^{\mathrm{i}\pi x_1/p}$ denoting the counter-propagating waves. For general structures the independent COM parameters are functions of position, but for the uniform structures used in this work they may be treated as constants. In such cases, the behavior of each

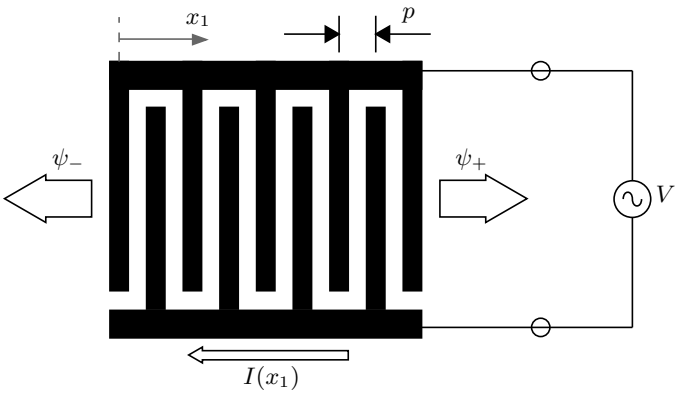

Fig. 1. IDT with COM wave parameters

structure at its acoustic ports $x_1 = b_1$ and $x_1 = b_2$ may be described using a P-matrix [19]:

$$\begin{bmatrix}\psi_-(b_1)\\ \psi_+(b_2)\\ I\end{bmatrix} = \begin{bmatrix}P_{11}(f) & P_{12}(f) & P_{13}(f)\\ P_{21}(f) & P_{22}(f) & P_{23}(f)\\ P_{31}(f) & P_{32}(f) & P_{33}(f)\end{bmatrix}\begin{bmatrix}\psi_+(b_1)\\ \psi_-(b_2)\\ V\end{bmatrix} \tag{2}$$

Expressions for the P-matrix elements are provided in [13], with alternative formulations given in [20]. The P-matrices of individual structures can then be cascaded to find the overall device response. For example, the total admittance $Y = G + \mathrm{i}B$ of a 1-port resonator with arbitrary P-matrix elements using cascading and reciprocity relations may be found from:

$$\begin{bmatrix}0\\ 0\\ Y\end{bmatrix} = \begin{bmatrix}(P_{11}P_{22}^r - 1) & P_{12}P_{11}^r & P_{13}\\ P_{12}P_{22}^r & (P_{22}P_{11}^r - 1) & P_{23}\\ -2P_{13}P_{22}^r & -2P_{23}P_{11}^r & P_{33}\end{bmatrix}\begin{bmatrix}\frac{\psi_-(x_1)}{V}\\ \frac{\psi_+(x_2)}{V}\\ 1\end{bmatrix} \tag{3}$$

The r superscript refers to the P-matrix elements of the reflector gratings; all others belong to the IDT. The Y expression in (3) can be evaluated analytically for bidirectional structures, enabling very fast calculation of a device's frequency response. In general, however, numerical methods must be used for more complicated devices, including those with more than one transducer and those using asymmetric structure designs and/or SAW propagation directions. Such cascading of device elements ensures that the model can simulate a wide variety of designs.

The modeling approach used in this work is to implement the effects of applied biases on the independent COM parameters and the device geometry, rather than on the basic COM model itself [16]. The layered SAW sensor modeling detailed in [14] uses an analogous technique, though this requires the use of Green's function and the boundary element method (BEM) to evaluate some of the COM parameters. While this approach has demonstrated good accuracy for layered devices, the computational requirements for such numerical methods can be considerable, especially when parametric studies are to be performed. The SAW pressure sensor described in [15] uses the COM model to evaluate the basic frequency response, though here the applied biases are not integrated into the COM parameters, nor are they used to predict device performance.

As the COM approach detailed above is general in nature, only minor additional assumptions are required to model externally applied biases:

- *Small loading effects*: the COM approach is based on perturbation theory, and thus the loading effects should be small. For example, large strain fields causing gross distortion of the substrate may introduce waveguiding effects which would not be modeled. This is generally not an issue for SAW sensors as they are limited to small strains due to the brittle nature of the substrates. Other biasing effects (e.g., from thermal or electrical fields) may be included through the higher-order coefficients of the substrate material if required.
- *Homogeneous biasing fields within each COM structure*: as mentioned above, the COM parameters are constants for uniform, unbiased structures. To retain this relationship, it is useful to assume that the biasing fields within each structure are also uniform. Even if the applied biases on the substrate are homogeneous, some stress concentrations may occur at the electrode-substrate interfaces due to the deposited structures, but the effects of these are included within the COM parameters. It would be possible to split the P-matrices of the structures into regions where individual loading effects are present and then use cascading [14], but this was considered unnecessary here as small biasing field gradients are assumed. The basic COM model already allows each structure to have different properties, and thus the biasing fields in a reflector grating, for example, may be different from those in the IDT.

It should be noted that, given the general nature of biased electroelastic analysis [21], it is often prudent to analyze a particular category of biases; only mechanical biases will be considered in this work as strain measurement is the target application. Extensions for thermal biases have been excluded for brevity, but may be added in a straightforward manner similar to that used in [10].

III. Model parameters

The determination of the independent COM parameters is a key aspect of any COM model. This is most commonly performed using perturbation methods [13], experimental fitting of actual device responses [22] or numerical methods [23]. The perturbation approach was chosen in this work in order to investigate the COM parameters individually at a low computational cost, thus demonstrating the effect of each parameter (and its sensitivity) on the sensor's frequency response. The following subsections detail the biased device geometry and the COM parameters. It should be noted that the COM model only simulates the SAW propagation region, and thus other parasitic factors in the device response (e.g., from IDT busbars, bond wires etc.), as well as the device resistance, must be treated separately. The surface waves are assumed to propagate in the x_1 direction, with x_2 as the surface normal.

A. Biased geometry

The COM model requires the width a and height h of each electrode, the SAW wavelength λ, the aperture W and structure length L. For the IDTs designs used in this project $\lambda = 2p = 4a$ and $L = Np$, where N is the number of periods. The strain due to the applied mechanical bias is given by the generalised Hooke's law:

$$S_{ij} = s_{ijkl} T_{kl} \tag{4}$$

where S_{ij} is the strain due to applied loads and the s_{ijkl} are the compliances of the substrate material; tensor summation has been assumed [6]. The substrate stress T_{kl} depends on the loading conditions of the substrate, which is assumed to be known from finite element [9] or other methods. S_{ij} is used to find the strained values of a, h and W, which are related to the other dimensions as above.

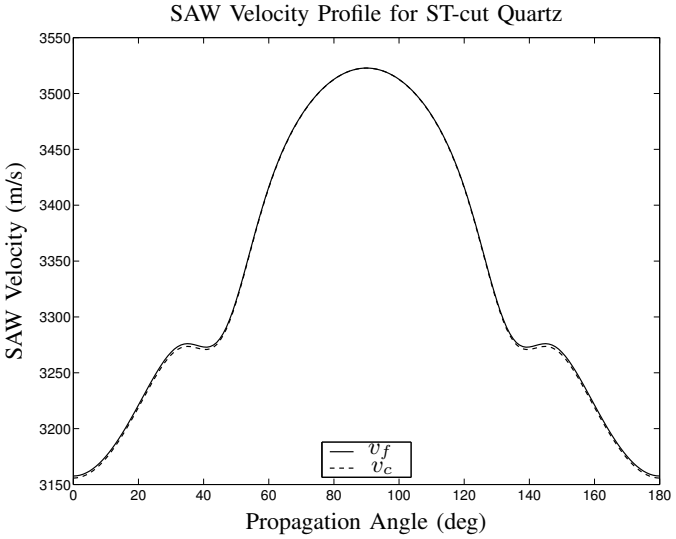

Fig. 2. SAW velocity as function of propagation angle on ST-cut quartz

B. SAW velocity

For homogeneous biases, the SAW velocity may be calculated using the procedure outlined in [24]. Fig. 2 plots the unbiased SAW velocities for free (v_f) and conducting (v_c) boundary conditions on ST-cut quartz, a common substrate for SAW strain and pressure sensors. A related parameter is the piezoelectric coupling coefficient K^2, which may be approximated as:

$$K^2 \approx \frac{2(v_f - v_c)}{v_f} \tag{5}$$

Fig. 3 plots K^2 for ST-cut quartz. The effects of applied biases may be included as per [6]. It should be noted that this method calculates the 'natural' velocity v_n [25], which takes into account both the change in the actual wave velocity and the propagation path. The actual fractional change in velocity for x_1 propagation is given by [26]:

$$\frac{\Delta v}{v} = \frac{\Delta v_n}{v} + S_{11} \tag{6}$$

Although biased velocity results are usually given as natural velocities (and thus $\Delta v_n / v = \Delta f / f$), here actual velocity sensitivities will be presented. This is done in order to separate

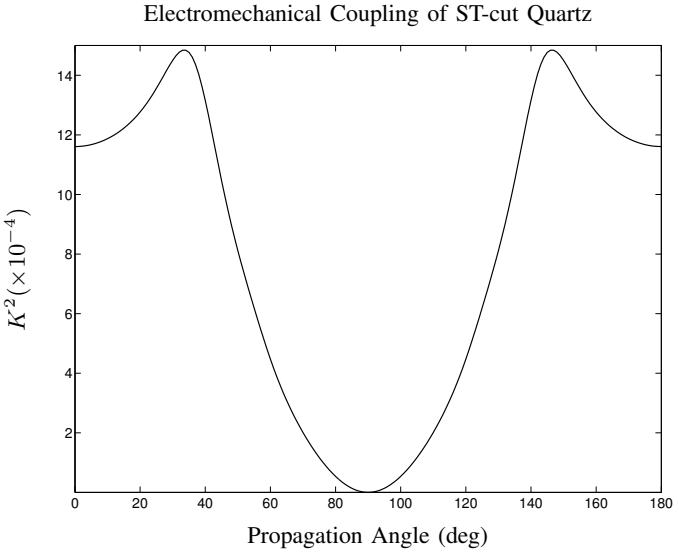

Fig. 3. SAW electromechanical coupling as function of propagation angle on ST-cut quartz

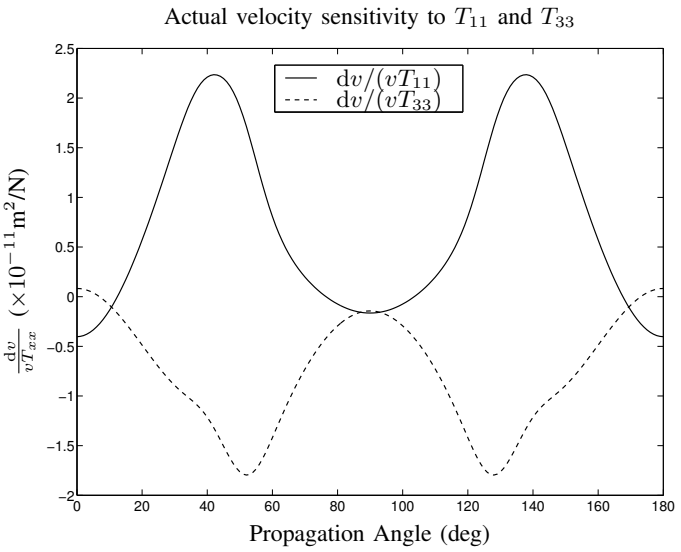

Fig. 4. Actual velocity sensitivity to T_{11} and T_{33} for ST-cut quartz

the effects of geometry change from those due to changes in propagation properties, as required by the COM model used here.

In general, mechanical biases on SAW strain sensors generate biaxial stress states [9], and thus the velocity sensitivities to axial (i.e., $\mathrm{d}v/(vT_{11})$) and transverse ($\mathrm{d}v/(vT_{33})$) stresses need to be evaluated. Fig. 4 plots these quantities for ST-cut quartz, demonstrating the variation in sensitivities with propagation direction. These can subsequently be superposed for a particular stress state. While this method can model the change in free-surface SAW velocity, the effect of the deposited structures must also be considered. This velocity change due to a periodic array of thin electrodes may be described as a power series expansion on the relative electrode thickness [13], [27], [28]:

$$\frac{\Delta v}{v} \approx \left(\frac{\Delta v}{v}\right)_e \left(\frac{K^2}{2}\right) + \left(\frac{\Delta v}{v}\right)_{m1} \left(\frac{h}{\lambda}\right) + \left(\frac{\Delta v}{v}\right)_{m2} \left(\frac{h}{\lambda}\right)^2 + \cdots \tag{7}$$

where:

$$\left(\frac{\Delta v}{v}\right)_e = -\frac{1}{2}\left(1 + \frac{L_{0.5}(-\cos(\pi\eta))}{L_{-0.5}(-\cos(\pi\eta))}\right) \tag{8}$$

$$\left(\frac{\Delta v}{v}\right)_{m1} = \frac{\eta\pi K^2}{C_n}\left(\left|\frac{u_1}{\varphi}\right|^2 (c_1 - \rho' v^2) - \left|\frac{u_2}{\varphi}\right|^2 \rho' v^2 + \left|\frac{u_3}{\varphi}\right|^2 (c_2 - \rho' v^2)\right) \tag{9}$$

In the above expressions, $L_n(x)$ is the Legendre function of order n, $\eta = a/p$ is the metallization ratio, C_n is the normalized capacitance (see below), u_i are the SAW displacement components, φ is the free-surface potential, c_1 and c_2 are related to the Lamé constants of the electrode material and ρ' is the density of the electrode material. An advantage of this particular form is that the biasing effects are naturally included in u_i and φ through the calculation of the biased velocity referenced to the unbiased state [5], [24], as is the anisotropy of the substrate. $(\Delta v/v)_{m2}$ may be calculated from a separate perturbation method [29], [30]. There are, however, significant differences between the calculated $(\Delta v/v)_{m2}$ values presented in [30] and the limited experimental measurements available (e.g., in [12]), thus it is preferable to calculate $(\Delta v/v)_{m2}$ experimentally.

C. Electrode reflectivity

In a similar manner to that used for the effects of electrodes on the COM velocity, the reflectivity of a periodic array may be described by a power series expansion on the relative electrode height [13], [27], [31]:

$$\kappa \approx \frac{1}{p}\left((\kappa)_e \left(\frac{K^2}{2}\right) + (\kappa)_{m1}\left(\frac{h}{\lambda}\right)\sin(\pi\eta) + \cdots\right) \tag{10}$$

where:

$$(\kappa)_e = -\frac{\pi}{2}\left(\cos(\pi\eta) + \frac{L_{0.5}(-\cos(\pi\eta))}{L_{-0.5}(-\cos(\pi\eta))}\right) \tag{11}$$

$$(\kappa)_{m1} = -\frac{\pi K^2}{C_n}\left(\left(\frac{u_1}{\varphi}\right)^2 (c_1 + \rho' v^2) + \left(\frac{u_2}{\varphi}\right)^2 \rho' v^2 + \left(\frac{u_3}{\varphi}\right)^2 (c_2 + \rho' v^2)\right) \tag{12}$$

Previous work has demonstrated that expansions of κ to first order are usually sufficiently accurate [31]. It should be noted that, unlike $\Delta v/v$, $(\kappa)_{m1}$ (and thus κ) may be complex. Fig. 5 shows the real and imaginary components of $(\kappa)_{m1}$ for ST-cut quartz, demonstrating the considerable variation in reflective behavior with propagation angle. The effect of

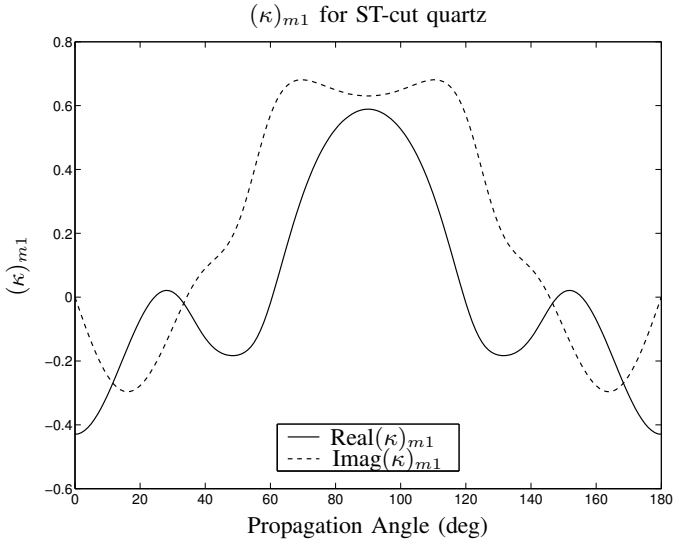

Fig. 5. $(\kappa)_{m1}$ for ST-cut quartz

biasing mechanical fields can be implemented in a similar manner to those in $(\Delta v/v)$, and thus κ can be made sensitive to biases.

The reflectivity parameter illustrates the importance of considering the behavior of both the device and the propagating waves when designing SAW sensors. Analysis of Fig. 3 indicates that maximum piezoelectric coupling is achieved for ST-(X+34°) propagation on this wafer cut, and from Fig. 4 the velocity sensitivities are relatively high: both of these suggest a useful sensor orientation. However, Fig. 5 shows that $(\kappa)_{m1}$, which is the dominant component of κ for this substrate, is virtually minimized for this orientation. This would lead to poor resonant performance using standard SAW resonator designs (see Section IV). Knowledge of the reflectivity behavior has previously been used to offset the small coupling of NSPUDT devices [32], and the same principle may be applied to SAW sensor design where the requirements of sensor sensitivity and resonant performance must be balanced.

D. Transduction coefficient

The transduction coefficient α determines the coupling between the excited SAW and the applied voltage. This may be decomposed into components related to the substrate properties, the SAW aperture and the electrode layout [33]. For the IDTs used in this work, the magnitude of α as a function of the wavenumber $\beta = \omega/v$ is given by:

$$|\alpha(\beta)| = \frac{|Q_F(\beta)|}{\lambda}\sqrt{\left(\frac{W}{\lambda}\right)\left(\frac{\pi(v_f - v_c)}{\varepsilon_s(\infty)}\right)} \qquad (13)$$

where $\varepsilon_s(\infty)$ is the effective permittivity of the substrate at infinite slowness [34], [35]. The IDT element factor $Q_F(\beta)$ details the electrostatic charge contribution of a single IDT 'cell' [33], and for the IDTs used here is given by [36]:

$$Q_F(\beta) = 2\varepsilon_s(\infty)\frac{L_m(\cos(\pi\eta))}{L_{-s}(-\cos(\pi\eta))}\sin(\pi s) \qquad (14)$$

where $m + s = \beta p/(2\pi)$, m is an integer and $0 \leq s \leq 1$. The phase of α is determined by that of $Q_F(\beta)$. The inclusion of $\varepsilon_s(\infty)$, v_f, v_c and the device geometry means that bias sensitivity of α can be evaluated: this is generally small relative to the orientational sensitivity plotted in Fig. 3.

E. Capacitance

The IDT electrodes in a SAW device act as distributed capacitors, and thus capacitive effects must be considered in the COM model. For weakly piezoelectric materials such as quartz, the normalized capacitance of the IDT may be approximated by its static capacitance:

$$C = \frac{C_n W}{\lambda} \qquad (15)$$

where C_n is the capacitance per electrode pair per unit aperture length [12]. For the IDTs used in this project, C_n may be determined from [34]:

$$C_n = \varepsilon_s(\infty)\frac{L_{-0.5}(\cos(\pi\eta))}{L_{-0.5}(-\cos(\pi\eta))} \qquad (16)$$

Unlike some of the other COM parameters, C_n is only weakly dependent on the propagation direction, though it does increase almost linearly with η around $\eta = 0.5$. As with most of the other COM parameters, the dependence of C on the device geometry (and on $\varepsilon_s(\infty)$) renders it sensitive to applied biases.

F. Attenuation

In the COM formulation, γ accounts for all of the acoustic loss mechanisms in a structure. For ST-X quartz, the COM free-surface attenuation is given by [34]:

$$\gamma \approx \frac{0.47 + 2.62 \times 10^{-9} f}{8685.9\lambda} \qquad (17)$$

where γ is measured in Nepers (1 Neper $\approx$ 8.6859 dB): the equation is sensitive to biases through λ as above. In addition, however, this parameter must also include losses from other sources (e.g., surface defects, bulk wave parasitic modes etc. [13]), which are difficult to model near the frequency ranges of interest. Losses from beam steering and diffraction should also be considered [34]. Recent work [37] has proposed more complete attenuation modeling, but in practice this parameter is usually measured experimentally.

IV. Example application

As an example application of the COM model, the measured behavior of an unbiased synchronous 1-port SAW resonator (SAWR) using ST-X propagation was compared against theoretical predictions. The measured COM parameters, which were fitted to an experimental response with excellent correlation, were presented in [38]. Table I compares these fitted values against those calculated in Section III; the p subscripts denote the COM parameters normalized to a unit period [13]. The following may be noted:

- The predicted v is larger than the measured value, primarily due to the omission of the $(\Delta v/v)_{m2}$ term from

TABLE I
COMPARISON OF FITTED COM PARAMETERS AND CALCULATED VALUES FOR SYNCHRONOUS 1-PORT SAW RESONATOR

Parameter	Fitted Value [38]	Calculated Value
v (m/s)	3146	3152
κ_p	-0.015	-0.021
$\alpha_p(\beta_0)$ ($\sqrt{1/\Omega\lambda}$)	2.71×10^{-4}	2.84×10^{-4}
C (pF)	1.95	1.92
R (Ω)	21.6	–
γ_p (Neper/λ)	3.82×10^{-4}	1.74×10^{-4}

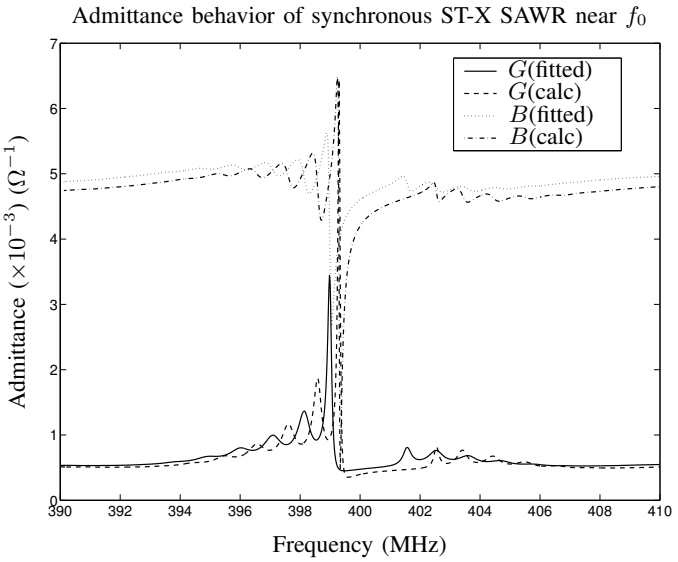

Fig. 6. Admittance behavior of a synchronous ST-X SAWR near f_0 using fitted and calculated COM parameters. Device parameters were taken from [38].

(7), as discussed above. Including a measured value of this term ($(\Delta v/v)_{m2} = -7.9$ [12] for the ST-X quartz orientation used in [38]) produces $v = 3142$m/s.

- The theoretical $|\kappa_p|$ is significantly larger than the fitted value, though more accurate predictions have been found in other studies (e.g., [31]).
- Simulated values of α_p and C are in good agreement with [38]. The experimental value of the resistance R is determined from the broadband response.
- As expected, the theoretical value of γ_p is smaller than that measured as only free-surface attenuation has been modeled.

Fig. 6 compares the modeled frequency responses using both sets of COM parameters; the fitted value of R is used in both cases. The larger theoretical reflectivity and lower attenuation lead to an overestimation of the resonant response magnitude. Similarly, the differing velocities cause a shift in the resonant frequency, defined here as $\max(G)$. In general, however, the theoretical parameters give a reasonable indication of device performance at a low computational cost, which is sufficient for a parametric study.

As a comparison, the performance of an identical device using ST-(X+34°) propagation, rather than the ST-X propagation used above, has been simulated. v, κ_p, α_p and C have been

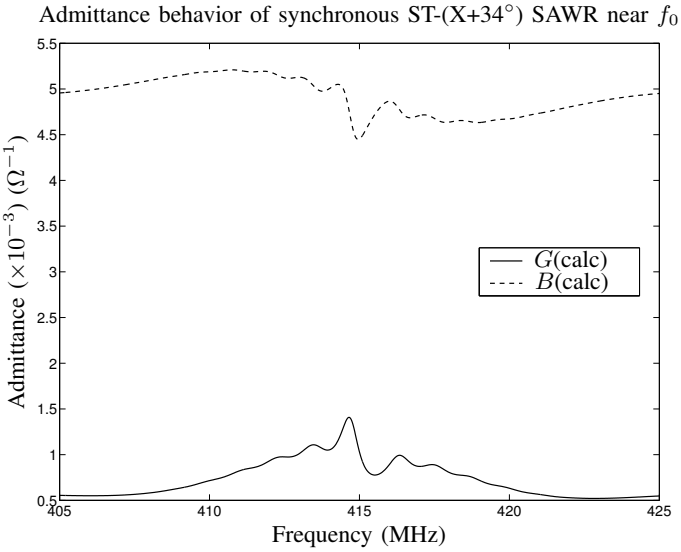

Fig. 7. Calculated admittance behavior of a synchronous ST-(X+34°) SAWR near f_0. Device parameters taken from [38].

TABLE II
CALCULATED RESONANT FREQUENCY SENSITIVITIES OF 1-PORT SYNCHRONOUS SAW RESONATOR TO APPLIED STRESSES FOR DIFFERENT PROPAGATION DIRECTIONS

Parameter	ST-X prop.	ST-(X+34°) prop.
$\mathrm{d}f/(fT_{11})$ ($\times 10^{-11}$ Pa^{-1})	-1.66	0.97
$\mathrm{d}f/(fT_{33})$ ($\times 10^{-11}$ Pa^{-1})	0.45	-0.98

calculated as above, while R and γ_p are assumed to be the same as the ST-X case for simplicity. The modeled resonant response is plotted in Fig. 7, which is clearly inferior to those shown in Fig. 6. As mentioned in Section III, this is because of the low κ value of this orientation, even though K^2 is maximized. The resonant frequency is also shifted due to the change in v.

As mentioned in Section I, the resonant frequency of the sensor device is often the primary measurand, and thus its bias sensitivity must be evaluated. Table II compares the calculated frequency sensitivities to axial and transverse stresses for the device detailed in [38] for different propagation directions. For SAWR subject to applied stresses, the change in v is usually dominant and thus $\mathrm{d}f/(fT_{xx}) \approx \mathrm{d}v_n/(vT_{xx})$; numerical results for the ST-X orientation correspond to those presented in [9]. Similar behavior was noted in [14] for mass-loaded devices, though in general the bias sensitivity of the COM parameters depends on the type of applied bias.

There are significant differences between the sensitivities for different stress components and propagation directions. The device displays good T_{11} sensitivity and selectivity for ST-X propagation, while the magnitudes of the sensitivities are almost equal for ST-(X+34°) propagation. This behavior is particularly important in sensor designs where multiple SAWR with different propagation directions are used on the same biased substrate, e.g., to create the equivalent of a strain gauge rosette. Each SAWR provides only a scalar measurement (through its resonant frequency or phase shift) of the tensor strain field, and thus measurements from several different

SAWR are required to characterize the complete strain state. The biased COM model allows the bias sensitivity of each SAWR in a sensor to be evaluated, and thus the performance of the whole sensor can be optimized. As an example, the design of each resonator could be modeled to ensure that its response is detectable in the presence of other devices, e.g., in frequency shift and resonant magnitude. In addition, bias-insensitive devices may be evaluated in order to reduce the effects of parasitic biases on the primary measurand.

V. Conclusion

The modeling of SAW strain sensors is an important consideration both for sensor design and for the evaluation of complete measurement systems. In this paper an integrated modeling scheme for such devices using COM analysis has been demonstrated. Following a description of the core COM model, the modifications and assumptions required to incorporate biasing effects were described. The theoretical independent COM parameters were then detailed, illustrating how biasing effects may be incorporated within their definitions. An example application was finally described to show how the model may be used to predict device performance.

The modeling approach detailed in this work should lead to a more unified description of SAW strain sensor behavior, where biasing effects are combined with the general frequency response of the device. In addition, the general nature of the model should allow its application to a range of SAW sensor types (temperature, pressure etc.), with the particular biases applied to the COM parameters as above.

References

[1] A. Pohl, "A review of wireless SAW sensors," *IEEE Trans. Ultrason., Ferroelectr., Freq. Control*, vol. 47, pp. 317–332, Mar. 2000.

[2] J. Beckley, V. Kalinin, M. Lee, and K. Voliansky, "Non-contact torque sensors based on SAW resonators," in *Proc. IEEE Int. Freq. Control Symp. and PDA Exhib.*, 2002, pp. 202–213.

[3] A. Pohl, R. Steindl, and L. Reindl, "The "Intelligent Tire" utilizing passive SAW sensors - measurement of tire friction," *IEEE Trans. Instrum. Meas.*, vol. 48, pp. 1041–1046, Dec. 1999.

[4] A. Pohl and F. Seifert, "Wirelessly interrogable surface acoustic wave sensors for vehicular applications," *IEEE Trans. Instrum. Meas.*, vol. 46, pp. 1031–1038, Aug. 1997.

[5] J. C. Baumhauer and H. F. Tiersten, "Nonlinear electroelastic equations for small fields superposed on a bias," *J. Acous. Soc. Am.*, vol. 54, pp. 1017–1034, Oct. 1973.

[6] B. K. Sinha and H. F. Tiersten, "On the influence of uniaxial biasing stresses on the velocity of piezoelectric surface waves," in *Proc. IEEE Ultrason. Symp.*, 1976, pp. 475–479.

[7] H. F. Tiersten, "Perturbation theory for linear electroelastic equations for small fields superposed on a bias," *J. Acous. Soc. Am.*, vol. 64, pp. 832–837, Sep. 1978.

[8] D. Hauden, M. Planat, and J. J. Gagnepain, "Nonlinear properties of surface acoustic waves: applications to oscillators and sensors," *IEEE Trans. Sonics Ultrason.*, vol. SU-28, pp. 342–348, Sep. 1981.

[9] B. K. Sinha and S. Locke, "Acceleration and vibration sensitivity of SAW devices," *IEEE Trans. Ultrason., Ferroelectr., Freq. Control*, vol. UFFC-34, pp. 29–38, Jan. 1987.

[10] X. Zhang, F.-Y. Wang, and L. Li, "Optimal selection of piezoelectric substrates and crystal cuts for SAW-based pressure and temperature sensors," *IEEE Trans. Ultrason., Ferroelectr., Freq. Control*, vol. 54, pp. 1207–1216, Jun. 2007.

[11] C. C. W. Ruppel, W. Ruile, G. Scholl, K. C. Wagner, and O. Männer, "Review of models for low-loss filter design and applications," in *Proc. IEEE Ultrason. Symp.*, 1994, pp. 313–324.

[12] C. K. Campbell, *Surface Acoustic Wave Devices for Mobile and Wireless Communications*. San Diego: Academic Press, 1998.

[13] V. Plessky and J. Koskela, "Coupling-of-modes analysis of SAW devices," *Int. J. High Speed Elec. Sys.*, vol. 10, pp. 867–947, Dec. 2000.

[14] D. A. Powell, K. Kalantar-zadeh, and W. Wlodarski, "Spatial sensitivity distribution of surface acoustic wave resonator sensors," *IEEE Sensors J.*, vol. 7, pp. 204–212, Feb. 2007.

[15] K. Lee, W. Wang, G. Kim, and S. Yang, "Surface acoustic wave based pressure sensor with ground shielding over cavity on 41° YX $LiNbO_3$," *Jpn. J. App. Phy.*, vol. 45, pp. 5974–5980, Jul. 2006.

[16] B. Mc Cormack, D. Geraghty, and M. O'Mahony, "Modelling of surface acoustic wave strain sensors using coupling-of-modes analysis," in *Eurosensors XIX*, 2005.

[17] H. A. Haus and W. Huang, "Coupled-mode theory," *Proc. IEEE*, vol. 79, pp. 1505–1518, Oct. 1991.

[18] W. R. Smith, H. M. Gerard, J. H. Collins, T. W. Reeder, and H. J. Shaw, "Analysis of interdigital surface wave transducers by use of an equivalent circuit model," *IEEE Trans. Microw. Theory Tech.*, vol. MTT-17, pp. 856–864, Nov. 1969.

[19] G. Tobolka, "Mixed matrix representation of SAW transducers," *IEEE Trans. Sonics Ultrason.*, vol. SU-26, pp. 426–428, Nov. 1979.

[20] K. Hashimoto, *Surface Acoustic Wave Devices in Telecommunications: Modelling and Simulation*. Berlin: Springer, 2000.

[21] J. Yang and Y. Hu, "Mechanics of electroelastic bodies under biasing fields," *App. Mech. Rev.*, vol. 57, pp. 173–189, May 2004.

[22] V. P. Plessky and C. S. Hartmann, "Characteristics of leaky SAWs on 36-$LiTaO_3$ in periodic structures of heavy electrodes," in *Proc. IEEE Ultrason. Symp.*, 1993, pp. 1239–1242.

[23] J. Koskela, V. P. Plessky, and M. M. Salomaa, "SAW/LSAW COM parameter extraction from computer experiments with harmonic admittance of a periodic array of electrodes," *IEEE Trans. Ultrason., Ferroelectr., Freq. Control*, vol. 46, pp. 806–816, Jul. 1999.

[24] A. J. Slobodnik, E. D. Conway, and R. T. Delmonico, "Microwave acoustics handbook volume 1A: Surface wave velocities," Air Force Cambridge Research Laboratories, Tech. Rep. AFCRL-TR-73-0597, 1973.

[25] R. N. Thurston and K. Brugger, "Third-order elastic constants and the velocity of small amplitude elastic waves in homogeneously stressed media," *Phy. Rev.*, vol. 133, pp. A1604–A1610, Mar. 1964.

[26] B. K. Sinha and H. F. Tiersten, "On the temperature dependence of the velocity of surface waves in quartz," *J. App. Phy.*, vol. 51, pp. 4659–4665, Sep. 1980.

[27] D.-P. Chen and H. A. Haus, "Analysis of metal-strip SAW gratings and transducers," *IEEE Trans. Sonics Ultrason.*, vol. SU-32, pp. 395–408, May 1985.

[28] T. Thorvaldsson, "Analysis of the natural single phase unidirectional SAW transducer," in *Proc. IEEE Ultrason. Symp.*, 1989, pp. 91–96.

[29] S. Datta and B. J. Hunsinger, "An analysis of energy storage effects on SAW propagation in periodic arrays," *IEEE Trans. Sonics Ultrason.*, vol. SU-27, pp. 333–341, Nov. 1980.

[30] H. Robinson, Y. Hahn, and J. N. Gau, "A comprehensive analysis of surface acoustic wave reflections: second-order effects," *J. App. Phy.*, vol. 68, pp. 4426–4437, Nov. 1990.

[31] T. Thorvaldsson and B. P. Abbott, "Low loss SAW filters utilizing the natural single phase unidirectional transducer (NSPUDT)," in *Proc. IEEE Ultrason. Symp.*, 1990, pp. 43–48.

[32] M. P. da Cunha and A. Y. Nakano, "Comparison between ST-cut quartz 25° and -60° NSPUDT propagation directions," *IEEE Trans. Ultrason., Ferroelectr., Freq. Control*, vol. 49, pp. 820–826, Jun. 2002.

[33] B. P. Abbott, C. S. Hartmann, and D. C. Malocha, "Transduction magnitude and phase for COM modelling of SAW devices," *IEEE Trans. Ultrason., Ferroelectr., Freq. Control*, vol. 39, pp. 54–60, Jan. 1992.

[34] D. P. Morgan, *Surface-Wave Devices for Signal Processing*. Amsterdam: Elsevier, 1985.

[35] R. F. Milsom, N. H. C. Reilly, and M. Redwood, "Analysis of generation and detection of surface and bulk acoustic waves by interdigital transducers," *IEEE Trans. Sonics Ultrason.*, vol. SU-24, pp. 147–166, May 1977.

[36] S. Datta and B. J. Hunsinger, "Element factor for periodic transducers," *IEEE Trans. Sonics Ultrason.*, vol. SU-27, pp. 42–44, Jan. 1980.

[37] S. Lehtonen, V. P. Plessky, C. S. Hartmann, and M. M. Salomaa, "Extraction of the SAW attenuation parameter in periodic reflecting gratings," *IEEE Trans. Ultrason., Ferroelectr., Freq. Control*, vol. 52, pp. 111–118, Jan. 2005.

[38] T.-T. Wu, S.-M. Wang, Y.-Y. Chen, T.-Y. Wu, P.-Z. Chang, L.-S. Huang, C.-L. Wang, C.-W. Wu, and C.-K. Lee, "Inverse determination of coupling of modes parameters of surface acoustic wave resonators," *Jpn. J. App. Phy.*, vol. 41, pp. 6610–6615, Nov. 2002.

Brian Mc Cormack (S'03) received the B.A., B.A.I. degree in mechanical and manufacturing engineering from Trinity College Dublin in 2002. He is now working towards the Ph.D. degree at the Centre for Transportation Research and Innovation for People (TRIP) at Trinity College Dublin.

His major research interest is in the development of surface acoustic wave devices for physical sensing, including their design and simulation.

Dermot Geraghty is a Lecturer in mechanical engineering at Trinity College Dublin. He is a graduate of Trinity College and holds the B.A., B.A.I. and M.Sc. degrees in engineering.

He leads a number of research projects in the development of sensors for transportation and environmental applications. He also works on the development of hardware architectures for high performance computing on field programmable gate arrays (FPGAs). He is a member of the Institution of Engineers of Ireland and the Association for Computing Machinery.

Margaret O'Mahony is the Professor of Civil Engineering at Trinity College Dublin. She also holds the position of Head of the Department of Civil, Structural and Environmental Engineering and Director of the Centre for Transport Research at TCD. A graduate of the National University of Ireland, Galway in civil engineering, she holds a doctoral degree in engineering science from the University of Oxford.

She leads a large number of interdisciplinary transport research projects, funded by the EU and other national research programmes. They focus on transport policy, ICT in transport, transport planning, network modelling, optimisation of transport networks, demand management, transport pricing, urban freight solutions, vehicle instrumentation and innovative road materials.